IOP PUBLISHING SCIENCE AND TECHNOLOGY OF ADVANCED MATERIALS

Sci. Technol. Adv. Mater. **9** (2008) 044102 (7pp) doi:10.1088/1468-6996/9/4/044102

TOPICAL REVIEW

Synthesis and superconducting properties of CaC_6

Nicolas Emery[1], **Claire Hérold**[1], **Jean-François Marêché**[1] **and Philippe Lagrange**[1,2]

[1] Laboratoire de Chimie du Solide Minéral—UMR 7555, Nancy Université, Université Henri Poincaré, BP 239, 54506 Vandœuvre-lès-Nancy Cedex, France
[2] Ecole Européenne d'Ingénieurs en Génie des Matériaux, Institut National Polyechnique de Lorraine, 6 rue Bastien Lepage, BP 630, 54010 Nancy Cedex, France

E-mail: Nicolas.Emery@live.fr and Claire.Herold@lcsm.uhp-nancy.fr

Received 10 October 2008
Accepted for publication 6 November 2008
Published 28 January 2009
Online at stacks.iop.org/STAM/9/044102

Abstract
Among the superconducting graphite intercalation compounds, CaC_6 exhibits the highest critical temperature $T_c = 11.5$ K. Bulk samples of CaC_6 are obtained by immersing highly oriented pyrographite pieces in a well-chosen liquid Li–Ca alloy for 10 days at 350 °C. The crystal structure of CaC_6 belongs to the $R\bar{3}m$ space group. In order to study the superconducting properties of CaC_6, magnetisation was measured as a function of temperature and direction of magnetic field applied parallel or perpendicular to the *c*-axis. Meissner effect was evidenced, as well as a type II superconducting behaviour and a small anisotropy. In agreement with calculations, experimental results obtained from various techniques suggest that a classical electron-phonon mechanism is responsible for the superconductivity of CaC_6. Application of high pressure increases the T_c up to 15.1 K at 8 GPa.

Keywords: graphite intercalation compound, synthesis, x-ray diffraction, crystal structure, superconductivity

(Some figures in this article are in colour only in the electronic version)

1. Introduction

Carbon exists in several allotropic forms including diamond, graphite, carbynes, fullerenes and carbon nanotubes. Graphite—a lamellar solid—is the most stable form at room conditions. It is built from sp^2 hybridised carbon atoms forming two-dimensional graphene layers connected by weak Van der Waals's bonds. The small carbon–carbon distance in the graphene planes (142 pm) originates from strong covalent bonds between adjacent carbon atoms. In reality, two bonds are stacked: a σ-bond and a π_z-bond. All the π_z-bonds belonging to the same graphene plane are delocalised on that plane. Weak Van der Waals bonds in the perpendicular direction result in much larger distance of 335 pm between the graphene planes.

Presence of strong covalent and weak Van der Waals bonds results in highly anisotropic properties of graphite. For this reason, soft chemical reactions take place, for which the chemical reagents can attack exclusively the areas of weak cohesion (called Van der Waals gaps), without disrupting the covalent bonds. These gaps (interplanar galleries) spread apart in order to accommodate the space necessary for setting up the reagent.

These specific soft reactions are called intercalation reactions. In most cases, they are reversible, and it is possible to regenerate the pristine graphite by a moderate heating. Because of its medium electronegativity, carbon acts as an amphoteric element, so that in intercalation reactions, graphite can provide or accept electrons. Electron transfer is compulsory for intercalation reactions.

Alkali metals, alkaline-earth metals and several lanthanides are very good reducing species; they intercalate into graphite at relatively low temperature, releasing electrons into the graphene layers and resulting in binary compounds [1–8].

Together with alkali metals, numerous other elements can intercalate into graphite producing ternary compounds. This category includes weakly electropositive elements H, Hg, Tl, Bi, As [9] and strongly electronegative O, S and halogens [10, 11]. All these elements behave towards graphite as electron donors (reducing agents) and generally result in poly-layered intercalated sheets.

The first measurement of superconductivity in a graphite intercalation compound was reported in 1965 [12] on KC_8 which exhibits very low critical temperature $T_c = 0.14$ K [13]. Later, several ternary graphite intercalation compounds revealed higher T_c of 1.4 K for $KHgC_8$ [14] and 2.7 K for $KTl_{1.5}C_4$ [15].

Recently, the discovery of high critical temperatures in graphite intercalation compounds YbC_6($T_c = 6.5$ K [16]), CaC_6($T_c = 11.5$ K [16, 17]) and $Li_3Ca_2C_6$ ($T_c = 11.15$ K [18]) has renewed the interest in this family of lamellar materials. This paper overviews synthesis, crystal structure and superconducting properties of CaC_6.

2. Synthesis

It is well established that intercalation of the alkaline earth metals from vapour phase into graphite is more difficult than of the alkali metals. Furthermore, among these metals, Ba and Sr intercalate rather easily as compared to Ca [6]—reaction between Ca vapour and a platelet of pyrolytic graphite leads only to a very superficial intercalation. Moreover the reaction temperature has to remain low enough to avoid formation of calcium acetylide. Consequently, bulk calcium–graphite materials have not been produced by vapour phase reaction, and their crystal structure and other properties have not been studied much.

In 2004, we have succeeded in synthesising CaC_6 in the bulk and almost pure form, using a novel method of plunging pyrolytic graphite into a molten Li–Ca alloy of certain composition [19]. We have shown that four factors are essential to the reaction: temperature, alloy composition, reaction time and purity of the reagents.

The reaction temperature is crucial because graphene planes are ruined above 450 °C. Fortunately, addition of Li to Ca decreases the high melting temperature of Ca (839 °C).

Reproducible reaction requires high purity of metallic reagents, which should be systematically handled in a glove box filled with high-purity argon. Both Li and Ca are precisely weighed to obtain an alloy with Li/Ca ratio between 3 and 4. Melting occurs in a stainless steel tube placed in a tubular vertical furnace, able to heat up to 400–450 °C. The alloy is then well agitated to obtain a homogeneous liquid.

A graphite platelet ($5 \times 15 \times 0.2$–0.5 mm) is then plunged into the molten alloy and the reactor is tightly closed under pure argon atmosphere. Finally, the reaction is carried out for ten days at around 350 °C. After this step, the sample is extracted from the reactor and its surface is cleaned by centrifugation at 300–350 °C or by cleavage. Rigorous observation of these experimental conditions results in pure first-stage CaC_6.

Intercalation mechanisms leading to CaC_6 was studied by x-ray diffraction (XRD) [20]. It is well established that the role of Li is twofold. Firstly, it serves as a flux for Ca, so that the liquid-solid reaction can be carried out at low temperatures. It also facilitates intercalation of Ca by pre-opening the graphitic galleries during the first step of the reaction. Indeed, during the first hour of the reaction, Li-graphite compounds follow successively through the 5th, 4th, 3rd, 2nd and 1st stages. This staging mechanism is quite usual for the intercalation reactions of pure metals into graphite. When the sample turns into quasi-pure LiC_6, the second mechanism begins, which is a slow and progressive substitution of Li by Ca, so that, after several days, the sample contains only pure CaC_6. During this slow substitution process, both LiC_6 and CaC_6 binaries coexist in the sample and total segregation of both compounds takes place.

3. Crystal structure

Synthesis of bulk CaC_6 by this novel technique greatly facilitated solving the CaC_6 crystal structure [21]. We know that at the first stage, binary graphite-metal intercalation compounds possess a very specific stoichiometry. Experimentally, we have shown that it corresponds to MC_8 for the biggest metals and to MC_6 for the smallest ones. When the interlayer distance exceeds 530 pm, the MC_8 stoichiometry is obtained (M = K, Rb and Cs), while the MC_6 (M = Li, Sr, Ba, Eu, Yb and Ca) composition is observed for smaller distances. The latter stoichiometry corresponds to an AAA... stacking of the successive graphene planes, so that the metal atoms are located in prismatic hexagonal sites, and the adjacent graphene and metal planes are epitaxial. In each graphitic gallery, only one out of three prismatic sites is occupied by a metal atom. Therefore, the metal plane can occupy three different positions in the graphitic interval (denoted α, β and γ, so that three different c-axis stacking possibilities can be considered [21] :

$$\begin{aligned} &A\alpha A\alpha A\alpha A\alpha A\alpha \ldots \\ &A\alpha A\beta A\alpha A\beta A\alpha \cdots \\ &A\alpha A\beta A\gamma A\alpha A\beta \ldots \end{aligned}$$

In the first case, the c parameter of the unit cell is obviously identical to the interlayer distance d_i, for the second stacking $c = 2d_i$, and for the third one $c = 3d_i$. The first or the second stacking leads to hexagonal crystal symmetry, and the third one corresponds to rhombohedral symmetry.

The first stacking was only observed for LiC_6; other known MC_6 compounds (SrC_6, BaC_6, EuC_6, SmC_6 and YbC_6) adopt the second stacking. As shown below, CaC_6 is different, and its rhombohedral symmetry agrees to the third stacking.

The x-ray diagram of the $00l$ reflections of CaC_6 gives interlayer distance of 452.4 pm (figure 1). Thanks to the

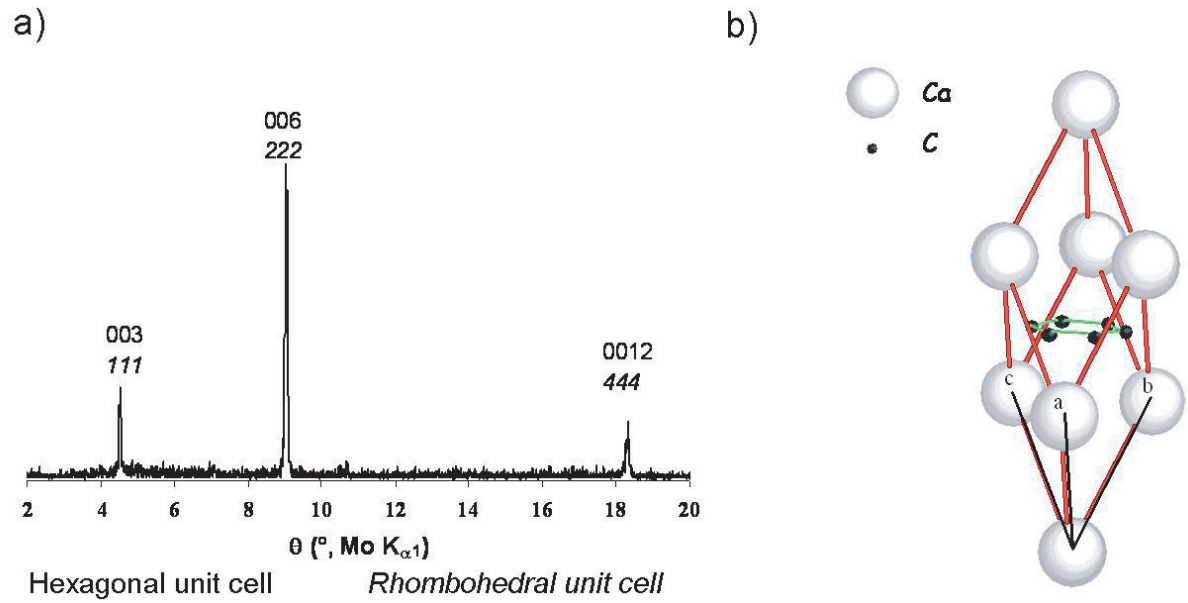

Figure 1. (a) 00*l* x-ray diffraction pattern. Reflexions are indexed in the hexagonal 00*l* and rhombohedral *hkl* representations (rhombohedral structure can be represented in both systems). (b) Crystal structure of CaC_6 (rhombohedral unit cell) [21].

drawing of its *c*-axis electronic density profile, the CaC_6 chemical formula is unambiguously established. At last, this stoichiometry was confirmed with high precision using nuclear microprobe [22, 23]. On the other hand, the study of the *hk*0 and *hkl* reflections also reveals its peculiar stoichiometry.

The diffraction pattern obtained by the rotating crystal method reveals the lattice parameter $a \cong 433$ pm. It is very close to $a_G\sqrt{3}$, where a_G corresponds to pristine graphite. This result additionally confirms the CaC_6 stoichiometry.

A detailed analysis of the [10] row of the diffraction pattern clearly shows that the *c* parameter of the 3D hexagonal unit cell reaches 1357.2 pm (three times of the interlayer distance: $1357.2 = 3 \times 452.4$) corresponding to the $A\alpha A\beta A\gamma A\alpha A\beta \ldots$ stacking.

Other observations have to confirm this interpretation. In particular, we have shown that the *hkl* reflections obey the general diffraction condition: $-h+k+l = 3n$. It is a good confirmation of the proposed model for the stacking of *c*-axis Ca planes. Such a stacking leads to rhombohedral symmetry (space group $R\bar{3}m$).

The description of CaC_6 in its rhombohedral unit cell leads to the following parameters: $a = 517$ pm, $\alpha = 49.55°$ (figure 1), and the Wyckoff's atomic positions are

C: 6 atoms 6*g* (1/6 5/6 1/2)
Ca: 1 atom 1*a* (0 0 0)

This unit cell is primitive, centrosymmetrical and belongs to the holoedry of the rhombohedral system.

The experimental *a* value was precisely determined from *hk*0 XRD pattern using diamond powder as internal standard. Therefore, the carbon-carbon distance in the graphene planes of CaC_6 can be calculated as 144.4 pm [21]. This distance is larger than in graphite due to intercalation; the difference reaches 2.4 pm or 1.69%. The Pietronero-Strässler formula allows to calculate the charge transfer due to intercalation of Ca into the graphitic galleries. The charge transfer per one carbon atom is 0.103. Interestingly, among all MC_6 compounds, CaC_6 shows the largest increase of C-C distance and strongest charge transfer.

In a recent work [24], metastable $CaSi_6$ compound was synthesised at pressure of 10 GPa and temperature of 1520 K. Under ambient conditions, $CaSi_6$ progressively turns into Si and $CaSi_2$. Although silicon and carbon belong to the same column of the periodic table, Si makes single bonds only, while carbon forms single, double and even triple bonds. In CaC_6, the carbon atoms are sp^2 hybridised so that the 2D graphene planes contain both single and double bonds which are delocalised in every successive plane. Calcium atoms intercalate between the planes so that their coordination by carbon is 6. On the contrary, in $CaSi_6$, the sp^3 hybridised Si atoms are connected by single bonds, leading to a 3D clathrate-like framework. This framework contains hexagonal cages, which embed Ca atoms with coordination by Si of 18. In both cases, Ca is ionised and the excess electrons are found in the basins of C–C or Si–Si covalent bonds. Electronic properties of CaC_6 and SiC_6 are very different: CaC_6 is metal and becomes superconducting at low temperatures, while SiC_6 is a poor conductor and is diamagnetic at low temperatures.

4. Superconducting properties

Since the discovery in 2005 of a superconducting transition in CaC_6 with T_c as high as 11.5 K [16, 17] (figure 2), much attention has been paid to alkaline-earth metal intercalated graphite. Two other superconductors were discovered, YbC_6 ($T_c = 6.5$ K [16]) and SrC_6 ($T_c = 1.65$ K [25]). In addition, surprisingly high T_c of 11.15 K was observed in ternary compound $Li_3Ca_2C_6$ [18]. Various experimental and theoretical studies attempted to explain the unusually high T_c

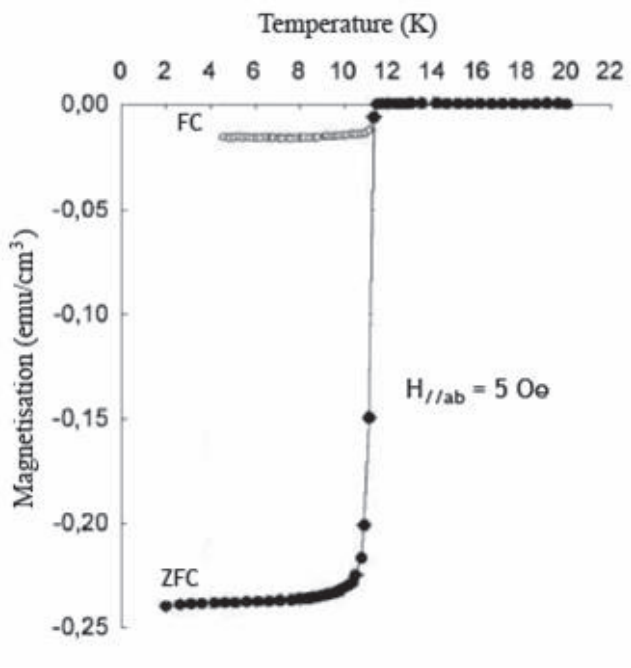

Figure 2. Zero field cooling (ZFC) and field cooling (FC) magnetisation versus temperature (field applied parallel to the graphene planes).

Table 1. Interlayer distances d_i, critical temperatures and anisotropic ratios of several graphite intercalation compounds.

Compound	d_i (pm)	$H_{c2\perp c}/H_{c2\parallel c}$	T_c (K)	Reference
KC_8	535	4.7–6.2	0.15	13
$KHgC_4$	1015	11	0.73	29
$KHgC_8$	1350	30–31	1.9	30
YbC_6	457	2	6.5	16
		2.1	6.5	31
$Li_3Ca_2C_6$	970	1.5	11.15	18
CaC_6	451		11.5	16
	452.4	2	11.45	17
		3.5–4	11.3	28

of these compounds as compared to the low T_c of traditional alkali metal-based graphite intercalation compounds (0.14 K for KC_8 [13] and 0.025 K for RbC_8 [26]). In this paper, we focus only on CaC_6, which was studied the most during the last 3 years.

Various magnetisation measurements [17, 27, 28] were performed to determine the critical fields in the two main orientations—with the external field perpendicular ($H_{\perp c}$) or parallel ($H_{\parallel c}$) to the graphite *c*-axis (figure 3). The upper critical fields $H_{c2\perp c}$ and $H_{c2\parallel c}$ reach 9500 Oe and 5000 Oe at 2 K, respectively [17], and the anisotropic ratio $H_{c2\perp c}/H_{c2\parallel c}$ is ∼2 [17, 24]. Slightly higher ratio was reported by Xie *et al* [28]. However, their sample was prepared by the vapour transport method, which leads only to a surface intercalation [4], and it showed lower T_c of 11.3 K. The anisotropic ratios of several graphite intercalation compounds are listed in table 1.

Despite the lamellar structure of such compounds, the magnetic behaviour of CaC_6 is more three-dimensional than expected. In comparison, superconducting potassium-based graphite intercalation compounds are more anisotropic. Quasi-2D superconductivity was however proposed for CaC_6 from magnetoresistance measurements [32]. Indeed, the angular dependence of the upper critical field is well fitted by the Lorentz–Doniach's theory, which assumes weak coupling between the superconducting layers in the 2D limit. A similar behaviour was recently observed for YbC_6 [31]. This behaviour can be explained by the thin-film nature of the sample, superficial intercalation and/or the high-density of stacking faults of the host graphite. Experiments on several samples, prepared from various kinds of graphite, are required to conclude on the evolution of the upper critical field. However, to our knowledge, it is not possible to obtain single crystals of graphite intercalation compounds due to the diffusive nature of the intercalation reaction—several domains are always created. The most studied example is KC_8, for which the polysynthetic nature was clearly demonstrated, even when the starting graphite was a single crystal [33].

Various theories have rapidly emerged to explain the surprisingly high T_c of CaC_6. One explanation is based on conventional electron–phonon pairing [34–37]; others [34] involve unconventional mechanisms such as plasmonic or excitonic pairing. The first experimental evidence was provided by high-resolution mutual inductance technique [38], which determined the symmetry of the gap function via magnetic penetration depth λ_{ab} in the superconducting state. In fact, λ_{ab} exhibits thermally activated behaviour, which can be related to an 's-wave' symmetry of the gap function (figure 4). This experimental result pointed to standard Bardeen–Cooper–Schrieffer's (BCS) scenario. The fit of $\Delta\lambda_{ab}$ (T) for $T < T_c/2$ leads to $\lambda_{ab}(0) = 72 \pm 8$ nm and a zero-temperature superconducting gap $\Delta(0) = 1.79 \pm 0.08$ meV. With these values, the ratio $2\Delta(0)/k_B T_c$ is estimated at 3.6 ± 0.2, which is very close to the BCS value of 3.52. Moreover, a good agreement with the calculation [35] is observed as the expected ratio reaches 3.69 [39], determined with the predicted value of electron–phonon coupling and the logarithmic average phonon frequency. Because of the CaC_6 atmospheric sensitivity, some oxide or hydroxide can be present on the surface. Measurements of $\Delta\lambda_{ab}$ on aged CaC_6 surface resulted in 30% lower gap value as compared to freshly cleaved samples [38].

During the nineties, it was believed that graphite intercalation compounds are two-gap superconductors [40]. In order to check this possibility, a fit of the data with a two-gap model [41] was attempted. However, no additional information was obtained, simply because single-gap analysis fully described the variation of $\Delta\lambda_{ab}$ [38].

Gap value $\Delta(0) = 1.5 \pm 0.3$ meV was reported [42] from microwave measurements. This slightly smaller value possibly relates to the smaller penetration depth of microwave impedance measurements and it confirms high surface reactivity of CaC_6.

The measured anomaly in the specific heat also suggests an s-wave gap with $2\Delta(0)/k_B T_c = 3.552$ [39]. However, Mazin *et al* [43] pointed out that the above-mentioned electron-phonon theories do not fit into these data. This problem was solved by recent calculations [44]. The method

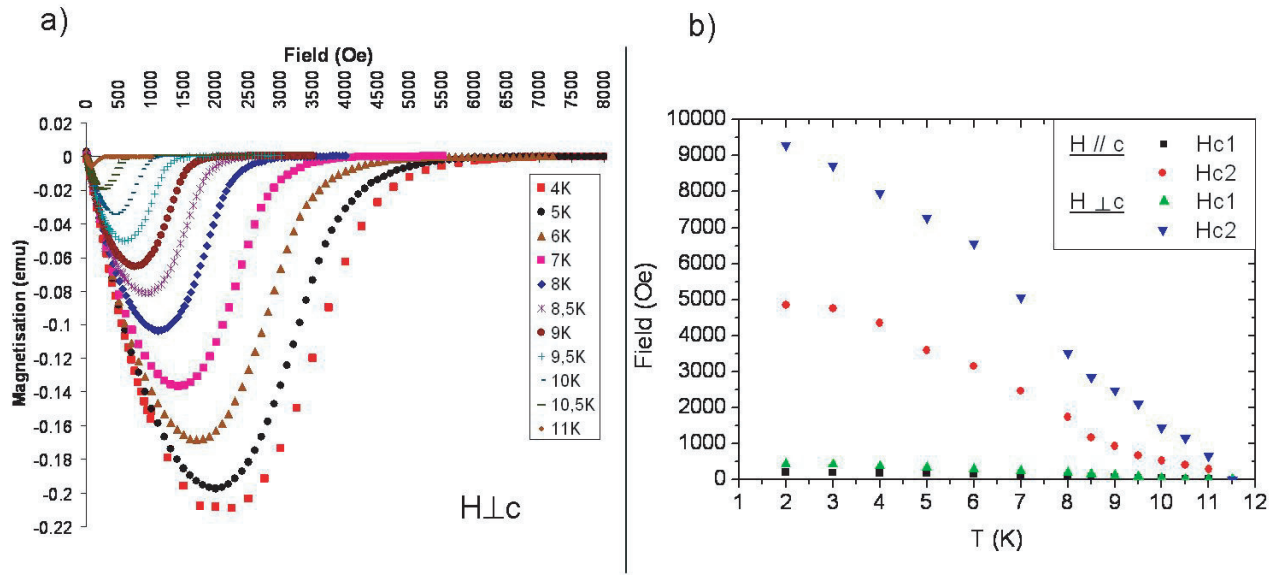

Figure 3. (a) Magnetisation versus field at various temperatures and (b) magnetic phase diagram of CaC_6 [17].

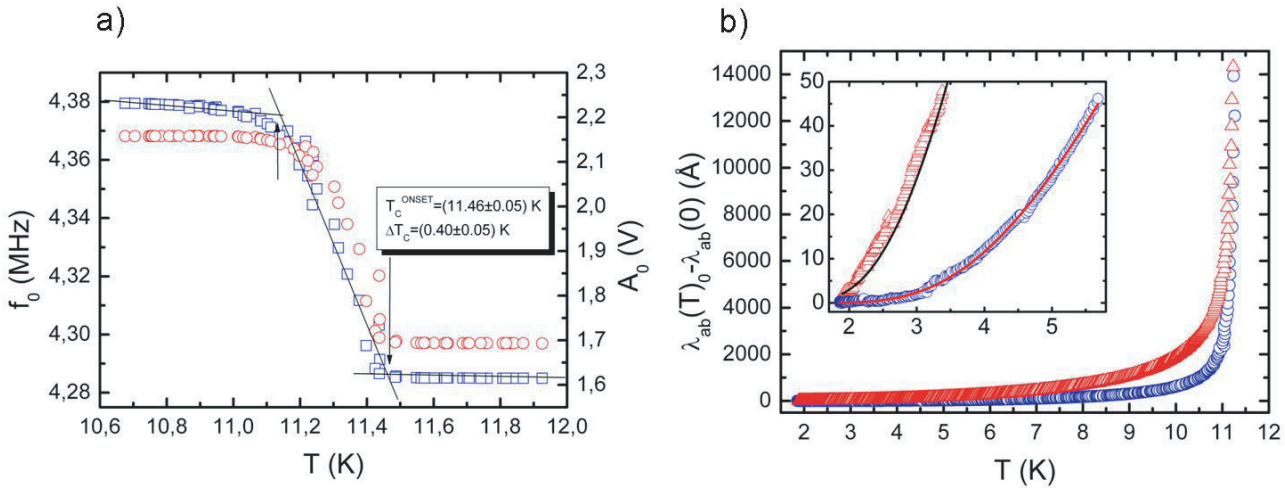

Figure 4. (a) Inductive characterisation of CaC_6 (resonance frequency f_0 and amplitude A_0), (b) variation of magnetic penetration depth $\Delta\lambda_{ab}$ with temperature. The inset zooms into low-temperature region (after [38]).

developed to describe superconductivity in elemental metals produced moderately anisotropic gap function perfectly fitting the specific heat measurements.

Scanning tunnelling microscopy and spectroscopy (STM/STS) [45] indicate a gap value $\Delta(0) = 1.6 \pm 0.2$ meV, in good agreement with the BCS theory. The coherence length in the *ab* plane, extracted from normalized zero-bias conductance vortex profile, reaches 33 nm, in good agreement with the value obtained from magnetic measurements [17]. No evidence of two-gap superconductivity is observed. A larger gap value $\Delta(0) = 2.3$ meV was reported by Kurter *et al* [46] suggesting possible strong coupling and anisotropic gap.

A clear proof of this anisotropy was given from directional point contact spectroscopy [47], which confirmed previous STM results and clearly showed the anisotropy of the gap function predicted by theory [44]. However, the gap value is 1.36–1.7 meV, and the anisotropy is probably greater than proposed from first-principles calculations. In addition to the STM experiments, far-infrared reflectance spectra [48] supported the s-wave scenario, confirming the anisotropy of the gap function.

5. Phonon properties

Phonon modes were studied by Raman scattering [49]. Spectra on cleaved surfaces systematically show two bands at 1500 cm^{-1} and 450 cm^{-1} assigned to Raman-active E_g modes originating from the in-plane bond-stretching mode and the out-of-plane puckering mode. The in-plane Ca modes might be accessible by far-IR absorption techniques.

An unusual Ca isotope effect coefficient of 0.52 was reported by Hinks *et al* [50]. This high value suggests low contribution of the C phonons to the superconducting mechanism. However, small amount of CaC_6 in the samples, due to the intercalation process, could also be a reason,

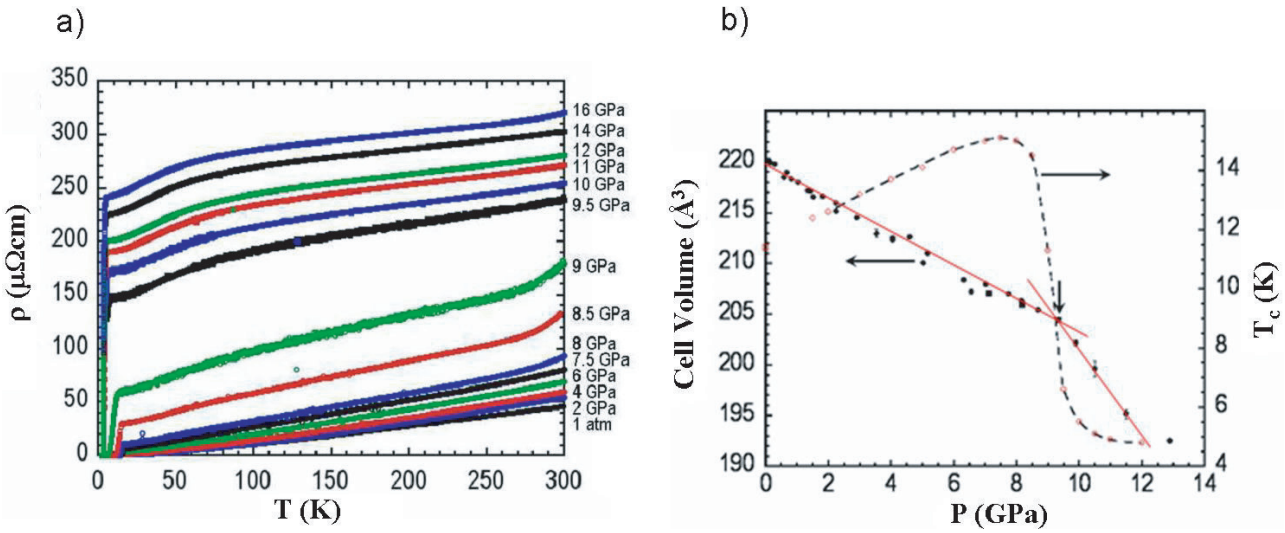

Figure 5. (a) Resistivity versus temperature under various pressures [51] and (b) evolution of the unit cell (hexagonal structure, left axis) and of the critical temperature (right axis) with pressure [55].

considering the smaller T_c observed in the ^{44}Ca-enriched sample. Nevertheless, recent calculations suggest that the Ca isotopic effect can be explained by the involvement of the Ca 3d states [51].

6. High pressure studies

High pressure is a powerful tool in studies of structural and superconducting properties. In case of CaC_6, T_c increase of 3.6 K is observed under a pressure $P = 8$ GPa [52] (figure 5). The T_c(P) dependence is linear, with a slope of $\sim$0.5 K GPa [52–54]. Generalized Bloch–Grueneisen's formula with two phonons modes fits the resistivity curves ρ(T) for $T > T_c$. The phonon energies and the weights of both modes at atmospheric pressure are in good agreement with the calculation [31]. In-plane Ca and out-of-plane C modes were attributed to the low- and the high-energy modes, respectively.

For pressure between 8 and 10 GPa, T_c dramatically falls to 5 K [52]. This phenomenon was attributed to the softening of the in-plane Ca phonon mode, leading to structural instability. Interestingly, YbC_6 exhibits a similar pressure dependence of the resistivity—T_c increases linearly first and then suddenly falls for $P > 2$ GPa [54].

X-ray diffraction measurements under pressures up to 13 GPa were carried out to understand this phenomenon [55]. No change in the space group and no extra peaks were observed. However, a clear change in the isothermal compressibility coefficient was detected (figure 5). Below 9 GPa, $da/dP = -0.38$ pm GPa^{-1} and $dc/dP = 8.1$ pm GPa^{-1}. At 9 GPa, the compressibility of CaC_6 suddenly increases by $\sim$3 times. In addition, a large increase of the XRD line width is observed for pressure above 9 GPa revealing pressure-induced disorder. Small displacement of Ca atoms might be responsible for this structural transition [56]. The associated symmetry reduction might be undetected due to insufficient signal-to-noise ratio.

7. Conclusions

Using a liquid-solid synthesis method, pure bulk samples of CaC_6 were prepared, allowing characterisation of structural and superconducting properties. CaC_6 crystallises in a rhombohedral unit cell (space group $R\bar{3}m$), and it is the only MC_6 type graphite intercalation compound adopting such a structure. CaC_6 is type-II superconductor with $T_c = 11.5$ K. This critical temperature is the highest for this class of materials. According to the various experiments and theories, the classical electron-phonon mechanism seems to be responsible for superconductivity. However, several points remain to be solved like, for example, the effect of graphite quality. Indeed, the amount of defects in the starting host material could be one of the causes of the small disagreements between various reports.

The critical temperature was increased up to 15.1 K by applying pressure of 8 GPa. At higher pressure, T_c falls dramatically. XRD has been recorded under pressure in order to understand the nature of this transition. No structural changes were detected and an order-disorder transition was pointed out.

References

[1] Fredenhagen K and Cadenbach G 1926 *Z. Anorg. Allg. Chem.* **158** 249
[2] Lagrange P, Guérard D and Hérold A 1978 *Ann. Chim. Fr.* **3** 143
[3] Lagrange P, Guérard D, El Makrini M and Hérold A 1978 *C.R. Acad. Sci. Paris* **287** 179
[4] Guérard D, Lagrange P, El Makrini M and Hérold A 1978 *Carbon* **16** 285
[5] Guérard D and Hérold A 1975 *Carbon* **13** 337
[6] Guérard D, Chaabouni M, Lagrange P, El Makrini M and Hérold A 1980 *Carbon* **18** 257
[7] El Makrini M, Guérard D, Lagrange P and Hérold A 1979 *Carbon* **18** 203
[8] Guérard D and Hérold A 1975 *C.R. Acad. Sci. Paris* **281** 929

[9] Lagrange P 1993 *Chemical Physics of Intercalation* II ed P Bernier *et al* (New-York: Plenum) 305 303–10
[10] Hérold C, Hérold A and Lagrange P 1996 *J. Phys. Chem. Solids* **27** 655
[11] Hérold C, Hérold A and Lagrange P 2004 *Solid State Sci.* **6** 125
[12] Hannay N B, Geballe T H, Matthias B T, Andres K, Schmidt P and Mac Nair D 1965 *Phys. Rev. Lett.* **14** 225
[13] Koike Y, Tanuma S, Suematsu H and Higuchi K 1980 *J. Phys. Chem. Solids* **41** 1111
[14] Pendrys L A, Wachnik R, Vogel F L, Lagrange P, Furdin G, El Makrini M and Hérold A 1981 *Solid State Commun.* **38** 677
[15] Wachnik R A, Pendrys L A, Vogel F L and Lagrange P 1982 *Solid State Commun.* **43** 5
[16] Weller T E, Ellerby M, Saxena S S, Smith R P and Skipper N T 2005 *Nat. Phys.* **1** 39
[17] Emery N, Hérold C, d'Astuto M, Garcia V, Bellin C, Marêché J F, Lagrange P and Loupias G 2005 *Phys. Rev. Lett.* **95** 087003
[18] Emery N, Hérold C, Marêché J F, Bellouard C, Loupias G and Lagrange P 2006 *J. Solid State Chem.* **179** 1289
[19] Pruvost S, Hérold C, Hérold A and Lagrange P 2004 *Eur. J. Inorg. Chem.* **1661**
[20] Emery N, Pruvost S, Hérold C and Lagrange P 2006 *J. Phys. Chem. Solids* **67** 1137
[21] Emery N, Hérold C and Lagrange P 2005 *J. Solid State Chem.* **178** 2947
[22] Pruvost S, Berger P, Hérold C and Lagrange P 2004 *Carbon* **42** 2049
[23] Berger P, Pruvost S, Hérold C and Lagrange P 2004 *Nucl. Instrum. Methods* B **219–220** 1005
[24] Wosylus A, Prots Y, Burkhardt U, Schnelle W and Schwarz U 2007 *Sci. Technol. Adv. Matter* **8** 383
[25] Kim J S, Boeri L, O'Brien J R, Razavi F S and Kremer R K 2007 *Phys. Rev. Lett.* **99** 027001
[26] Kobayashi M, Enoki T, Inokuchi M, Sano M, Sumiyama A, Oda Y and Nagano H 1985 *J. Phys. Soc. Japan* **54** 2359
[27] Kadowaki K, Nabemoto T and Yamamoto T 2007 *Physica* C **460–462** 152
[28] Xie R, Rosenmann D, Rydh A, Claus H, Karapetrov G, Kwok W K and Welp U 2006 *Physica* C **439** 43
[29] Chaiken A, Dresselhaus M S, Orlando T P, Dresselhaus G, Tedrow P M, Neumann D A and Kamitakahara W A 1990 *Phys. Rev.* B **41** 71
[30] Alexander M G, Goshorn M P, Guérard D, Lagrange P, El Makrini M and Onn M G 1981 *Solid State Commun.* **38** 103
[31] Kawai N F and Fukuyama H 2008 arXiv:0807.2706v1 [cond-mat]
[32] Jobiliong E, Zhou H D, Janik J A, Jo Y-J, Balicas L, Brooks J S and Wiebe C R 2007 *Phys. Rev.* B **76** 052511
[33] Lagrange P, Guérard D and Hérold A 1978 *Ann. Chim. Fr.* **3** 143
[34] Csányi G, Littlewood P B, Nevidomskyy A H, Pickard C J and Simons B D 2005 *Nat. Phys.* **1** 42
[35] Calandra M and Mauri F 2005 *Phys. Rev. Lett.* **95** 237002
[36] Kim J S, Kremer R K, Boeri L and Razavi F S 2006 *Phys. Rev. Lett.* **96** 217002
[37] Mazin I I 2005 *Phys. Rev. Lett.* **95** 227001
[38] Lamura G, Aurino M, Cifariello G, Di Gennaro E, Andreone A, Emery N, Hérold C, Marêché J-F and Lagrange P 2006 *Phys. Rev. Lett.* **96** 107008
[39] Marsiglio F, Carbotte J P and Blezius J 1990 *Phys. Rev.* B **41** 6457
[40] Al-Jishi R 1983 *Phys. Rev.* B **28** 112
[41] Lamura G *et al* 2002 *Phys. Rev.* B **65** 020506
[42] Andreone A, Cifariello G, Di Gennaro E, Lamura G, Emery N, Hérold C, Marêché J-F and Lagrange P 2007 *Appl. Phys. Lett.* **91** 072512
[43] Mazin I I, Boeri L, Dolgov O V, Golubov A A, Bachelet G B, Giantomassi M and Andersen O K 2007 *Physica* C **460–462** 116
[44] Sanna A, Profeta G, Floris A, Marini A, Gross E K U and Massidda S 2007 *Phy. Rev.* B **75** 020511R
[45] Bergeal N, Dubost V, Noat Y, Sacks W, Roditchev D, Emery N, Hérold C, Marêché J F, Lagrange P and Loupias G 2006 *Phys. Rev. Lett.* **97** 077003
[46] Kurter C, Oyuzer L, Mazur D, Zasadzinski J F, Rosenmann D, Claus H, Hinks D G and Gray D E 2007 *Phys. Rev.* B **76** 220502R
[47] Gonelli R S, Delaude D, Tortello M, Ummarino G A, Stepanov V A, Kim J S, Kremer R S, Sanna A, Profeta G and Massidda A 2007 arXiv:0708.0921 [cond-mat]
[48] Nagel U, Hüvonen D, Joon E, Kim J S, Kremer R K and Rõõm T 2008 *Phys. Rev.* B **78** 041404
[49] Hlinka J, Gregora I, Pokorny J, Hérold C, Emery N, Marêché J F and Lagrange P 2007 *Phys. Rev.* B 144512
[50] Hinks D G, Rosenmann D, Claus H, Bailey M S and Jorgensen J D 2007 *Phys. Rev.* B **75** 014509
[51] Deng S, Simon A and Köhler J 2008 *Angew. Chem. Int.* **47** 6703
[52] Gauzzi A, Takashima S, Takeshita N, Terakura C, Takagi H, Emery N, Hérold C, Lagrange L and Loupias G 2007 *Phys. Rev. Lett.* 067002
[53] Kim J S, Boeri L, Kremer R K and Razavi F S 2006 *Phys. Rev.* B **74** 214513
[54] Smith R P, Kusmartseva A, Ko Y T C, Saxena S S, Akrap A, Forró L, Laad M, Weller T E, Ellerby M and Skipper N T 2006 *Phys. Rev.* B **74** 024505
[55] Gauzzi A *et al* 2008 *Phys. Rev.* B **78** 064506
[56] Csànyi G, Pickard C J, Simons B D and Needs R J 2007 *Phys. Rev.* B **75** 085432